THE GEOLOGICAL SOCIETY OF AMERICA®

Asian collisional subduction: A key process driving formation of the Tibetan Plateau

Anne Replumaz[1]*, F. Funiciello[2], R. Reitano[2], C. Faccenna[2], and M. Balon[1]
[1]ISTerre (Institut des Sciences de la Terre), Université Grenoble Alpes, CNRS, F-38000 Grenoble, France
[2]Dipartimento Scienze, Università degli Studi, Roma TRE, Largo S. Leonardo Murialdo 1, 00146 Rome, Italy

ABSTRACT

Using silicone slabs as a model analogue for lithospheric plates subducting into a box of glucose syrup, as an analogue of the mantle, we explore the subduction of continental lithosphere in a context of intercontinental collision. The continental indenter pushed by a piston, reproducing the collision, attached to a dense oceanic plate, subducts to two-thirds of the depth of the mantle box. We show that, surprisingly, the continental plate attached to the back wall of the box subducts, even if not attached to a dense oceanic slab. The engine of this subduction is not the weight of the slab, because the slab is lighter than the mantle, but the motion of the piston, which generates horizontal tectonic forces. These are transmitted to the back wall plate through the indenter and the upper plate at the surface, and by the advancing indenter slab through the mantle at shallow depth. We define this process as collisional subduction occurring in a compressional context. The collisional subduction absorbs between 14% and 20% of the convergence, and represents an unexplored component of collisional mass balance. The transmission of tectonic forces far from the collision front favors the formation of a wide plateau. Our experiments reproduce adequately the amount and geometry of the Asian lithosphere subduction episodes inferred during the collision, leading us to conclude that it reproduces adequately the physics of such process.

INTRODUCTION

Several decades of seismic profiles and global tomography illuminate the lithospheric structure of the Tibetan Plateau, showing the subduction of the Asian continental lithosphere during the collision with India (Fig. 1). In the western syntaxis, the Asian lithosphere is subducting southward beneath Pamir down to 300–400 km (Negredo et al., 2007). In central Tibet, the Asian lithosphere is subducting southward down to 300 km (Kind et al., 2002). Cenozoic volcanic rocks between 50 and 30 Ma in the Qiangtang block have been interpreted as related to the subduction of the Asian lithosphere beneath Qiangtang during the early collision (DeCelles et al., 2002).

To the south, the Indian lithosphere subducts northward beneath the Hindu Kush facing the Asian slab beneath Pamir (Negredo et al., 2007; Kufner et al., 2016), and in the early time of the collision, facing the Asian slab beneath Qiangtang (DeCelles et al., 2002; Replumaz et al., 2013) (Fig. 1). The processes allowing the subduction of the Indian lithosphere have been widely explored. In particular, it has been shown that to sustain a high convergence rate of ~5 cm/yr for longer than 50 m.y., as observed for India and the strong thickening of the Tibetan Plateau, far-field forces have to be invoked (e.g., Becker and Faccenna, 2011; Capitanio et al., 2015). In analogue experiments, such far-field forces permit the deep subduction of the indenter continental slab and the indentation of the upper plate, with a shape of the suture compatible with the Himalaya-Tibet geometry (Bajolet et al., 2013).

One key conceptual problem not yet explored is what enhances the subduction of the Asian continental lithosphere in the mantle, without it being attached to an oceanic slab (Fig. 1). In this paper we explore the influence of the forces generated by a collision in the overriding plate on its subduction that we call collisional subduction. We also explore how this mechanism favors the development of the wide Tibetan plateau.

MODEL SETUP AND EXPERIMENTAL PROCEDURE

Model Setup

The experimental setting consists of 11 cm of glucose syrup, corresponding to the upper mantle in nature (660 km), on top of which there are three silicone plates (Table 1). The indenter plate is made of two silicones: a silicone lighter than the syrup reproducing a continental lithosphere (indenter), and a silicone denser than the syrup reproducing an oceanic lithosphere (ocean 1) (Fig. 2). The trailing edge of the light silicone is attached to a piston advancing at constant velocity. At the back wall of the box, the back wall plate is made of a light silicone, the trailing edge of which is fixed to the wall.

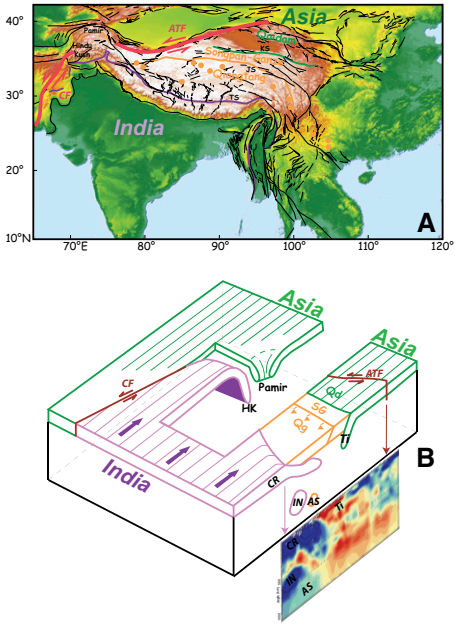

Figure 1. A: Topographic map of the collision zone between India and Asia. The Indian crust is separated from the Asian crust by the Tsangpo suture (TS, in purple). In central Tibet, the Qiangtang block is separated from the Songpan-Ganze block by the Jinsha suture (JS, in orange), separated from the Qaidam block (Qd) by the Kunlun suture (KS, in green). Orange points in the Qiangtang block are Cenozoic volcanic rocks between 50 and 30 Ma. ATF—Altyn Tagh fault; CF—Chaman fault. B: Three-dimensional schematic view of the lithospheric structure (middle-lower crust and lithospheric mantle) below Tibet showing along-strike variability. To the southeast, the Indian lithosphere (in purple) subducts northward beneath the Hindu Kush (HK) down to the transition zone (~600 km), facing the Asian lithosphere (in green) subducting beneath Pamir down to 300–400 km. In central Tibet, the Asian lithosphere (Ti, in green) is subducting southward below Songpan-Ganze (SG, in orange) down to 300 km, facing the Indian craton lithosphere (CR) underplating south Tibet. In the time of early collision, the Indian lithosphere (IN) has also subducted northward facing the Asian slab (AS) beneath Qiangtang (Qg). Both slabs have been detached from the continents and have sunk down to the lower mantle, as visible on the global tomographic cross section (Replumaz et al., 2013). The color code used for the different plates is also applied to the experimental data.

*E-mail: anne.replumaz@univ-grenoble-alpes.fr

TABLE 1. DIMENSION, DENSITY, AND VISCOSITY OF PLATES FOR THE THREE EXPERIMENTS

Experiment	Indenter	Ocean 1	Upper plate	Back wall plate	Ocean 2
1	20·25·1.1 cm^3	20·7·1.1 cm^3	20·10·0.8 cm^3	20·20·0.8 cm^3	
	ρ = 1402 kg/m^3	1508	1397	1402	
	$\mu = 2 \times 10^5$ Pa·s	3.3×10^4	2.9×10^4	2×10^5	
2	20·25·1.1 cm^3	20·7·1.1 cm^3	20·10·0.8 cm^3	20·20·0.8 cm^3	20·3·1.1 cm^3
	ρ = 1402 kg/m^3	1508	1397	1402	1508
	$\mu = 2 \times 10^5$ Pa·s	3.3×10^4	2.9×10^4	2×10^5	$3 \times 3\ 10^4$
3	20·25·1.1 cm^3	20·7·1.1 cm^3	20·10·0.8 cm^3	20·20·0.8 cm^3	
	ρ = 1402 kg/m^3	1508	967	1402	
	$\mu = 2 \times 10^5$ Pa·s	3.3×10^4	2.6×10^4	2×10^5	

Note: The glucose syrup, analogue of the mantle, has a density of 1428 kg/m3 and a viscosity of 30 Pa·s.

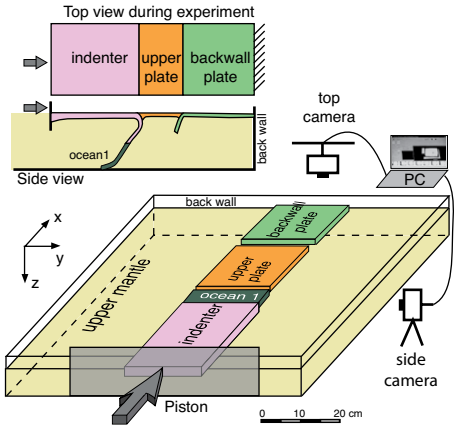

Figure 2. Experimental setup, three-dimensional view of the initial stage, and top and side views during experiment.

The leading edge of the back wall plate is either made of a dense silicone (ocean 2) similar to the indenting plate (experiment 2), or not (experiments 1 and 3). Between the indenting plate and the back wall plate, there is a third light silicone layer, the upper plate (Fig. 2).

The experiments are scaled for gravity, length, density, viscosity, and velocity. Each experiment is monitored over its entire duration by top and lateral view photos taken at regular time intervals (Fig. 2), which enables us to quantify the amount of subducted lithosphere, the thickening of the plates, and the displacement field (Appendix DR1 in the GSA Data Repository[1]).

Forces Equilibrium

Before the piston starts to move, the leading edge of the indenting oceanic plate and/or the back wall plate is curved manually downward inside the syrup. Then the model evolves in a self-consistent way with its dynamics controlled by the piston kinematics, mimicking the far field of a collisional system and the interplay between buoyancy and viscous forces of the entire system. With respect to the viscous forces the slab pull mirrors the slab buoyancy relative to the mantle, which is a function of the density contrast between lithosphere and mantle (e.g., Forsyth and Uyeda, 1975). For a dense oceanic lithosphere, the slab pull represents the main driving force of the system. However, when light continental lithosphere is subducted, the downward buoyancy and, in turn, the slab pull decreases. For the Indian case, in order to generate the fast convergence of India and the strong thickening of Tibet, mantle drag generated by a large-scale convection cell (Becker and Faccenna, 2011; Capitanio et al., 2015) that could be accelerated by slab avalanching in the lower mantle (Faccenna et al., 2013), or plume push (van Hinsbergen et al., 2005), must be invoked. In our experiments, we use a piston as analogue of such far-field forces.

EXPERIMENTAL RESULTS

We performed experiments to explore the parameters that control the subduction of a lithosphere lighter than the mantle in the context of continental collision (Appendix DR2). In this paper we present in detail the results of experiment 1, which is the most similar to what is currently observed beneath Tibet, showing the subduction of Asian continental lithosphere not attached to an oceanic slab (Fig. 1). We compare this experiment with (1) experiment 2, where the back wall plate is attached to an oceanic lithosphere, to explore the effect of a more efficient subduction process; and (2) experiment 3, where the upper plate is softer, to explore the effect of a more efficient deformation at the surface (Table 1).

Reference Experiment 1: Collisional Subduction of Continental Lithosphere

The convergence generated by the motion of the piston is absorbed first by the subduction of the indenting plate, then by both the subduction of indenter and back wall plate, and the deformation of the three plates (Fig. 3). At the beginning of the experiment, the oceanic slab attached to the indenter generates a positive slab pull, and the slab dips vertically, until it reaches the bottom of the box (time, t = 0 min). Then it pulls the light indenter into the mantle, the slab overturns (t = 30 min), and deforms a great deal (t = 50 min), until it touches the back wall slab (t = 70 min). The vertical component of velocity decreases rapidly before stopping (t = 30 min). Equilibrium occurs between the dense oceanic roots and the light indenter, plunging no deeper than about approximately one-half of the box. The back wall plate also subducts continuously but slower than the indenter (Fig. 3E). The slab pull is negative from the beginning of the experiment, as the plate is lighter than the mantle, and decreases as the slab length increases continuously. The slab is steep but not vertical, and reaches approximately one-third of the box depth.

The thickness increases continuously for the three plates (Fig. 3F). For the indenter, the thickness increases to ~134% at t = 50 min, and ~175% at t = 70 min. For the back wall plate, composed of the same silicone, the evolution is very similar, to ~137% at t = 50 min, and ~160% at t = 70 min. For the weaker upper plate, the thickness increases much more rapidly, and reaches a higher value, ~175% at t = 50 min, and ~238% at t = 70 min.

The horizontal velocity decreases from the piston to the back wall, as convergence is absorbed by subduction and thickening (Fig. 3B). At t = 50 min the convergence has been absorbed by the subduction of the indenter (17%–24%), its thickening (20%–25%), the subduction of the back wall plate (14%–18%), its thickening (16%–18%), and the thickening of the upper plate (~23%).

The use of silicone, which thickens by pure shear, does not adequately reproduce the complex thickening process of the Tibetan upper crust, which could be duplicated under Tibet by underthrusting (DeCelles et al., 2002), but silicone adequately simulates the subduction of the lithosphere and the overall lithospheric-mantle dynamics.

Experiment 2: Subduction of Continental Lithosphere Attached to Oceanic Lithosphere

In the second experiment, both the indenter and the back wall plate are attached to a dense oceanic slab. The overall behavior of the indenter slab is similar to that in the reference experiment (Fig. 4A). However, the back wall continental slab is much longer than in the reference experiment. It deepens down to about the two-thirds of the box, twice the length observed in the reference experiment. The back wall slab is vertical during the entire experiment, reaching the bottom of the box only at the end of the experiment (Fig. 4A). The thickness evolution of the back wall plate is similar than in the reference experiment. For the upper plate the thickening is reduced compared to the reference experiment, reaching only 143% at t = 50 min, instead of 175%. At t = 50 min the convergence has been absorbed by the subduction of the indenter (14%–23%), its thickening (21%–28%), the subduction of the back wall plate (~20%), its thickening (~16%), and the thickening of the upper plate (~17%).

[1]GSA Data Repository item 2016315, Appendices DR1 and DR2, is available online at www.geosociety.org/pubs/ft2016.htm, or on request from editing@geosociety.org.

Experiment 3: Collisional Subduction with Very Weak Upper Plate

In the third experiment, the upper plate is made of weak silicone, more easily deformable than the one used in the reference experiment (Table 1). In that case, the deformation of the upper plate increases. The upper plate thickens (171% at t = 50 min) similarly than in the reference experiment (175% at t = 50 min), but spreads laterally. A part of the plate is pushed laterally away from the frontal collision zone (Fig. 4C). The equivalent thickness without such extrusion would be 200% at t = 50 min.

In experiment 3, the indenter does not subduct in the mantle (Fig. 4C). At the beginning of the experiment the contact occurs between the upper plate and ocean 1, not between the upper plate and the indenter. The upper plate sticks to ocean 1, reducing the slab pull and slowing the subduction.

For the back wall plate, the slab length is slightly shorter for the reference experiment 1, and the thickening slightly reduced, only 131% (Fig. 4). At t = 50 min the convergence has been absorbed by the thickening of the indenter (~33%), its subduction (1%–3%), the subduction of the back wall plate (~20%), its thickening (~19%), and the thickening of the upper plate (~25%).

EXPERIMENTAL EVIDENCE OF COLLISIONAL SUBDUCTION

The most striking result is that the back wall plate in a context of collision subducts in our three experiments, even if it is lighter than the mantle (Fig. 3E). It subducts whether or not it is attached to a dense oceanic slab (Fig. 4). It subducts if the upper plate is weak or very weak. The engine of this behavior is not the slab pull, which is negative, but the motion of the piston, which generates horizontal tectonic forces. These are transmitted to the back wall plate through the indenter and the upper plate at the surface, and by the advancing indenter slab at shallow depth (Fig. 4). The subduction of the Asian plate is thus forced by the collisional setup, without any contribution given by oceanic lithosphere. Because subduction does not describe adequately this process, we use the phrase collisional subduction. Such collisional subduction occurs in a compressional context and is associated with thickening of the plates (Fig. 3F). Such forced subduction occurs along a suture, making a discontinuity in the upper plate. In experiments 1 and 2, the back wall plate is curved manually before the piston starts to move (Fig. 3A), reproducing the possible shape of the lithosphere along a suture. This configuration favors the initiation of the subduction. Nevertheless, if no preliminary curving of the back wall plate is made, subduction also occurs (experiment 3).

The collisional subduction absorbs a significant amount of convergence during the collision, between 14% and 20%, which makes this process, not yet explored, crucial during a collision. In the reference experiment, the amount of convergence absorbed is 14%–18% of the total convergence at t = 50 min (Fig. 4B). The slab reaches approximately one-third of the box, equivalent to 200–250 km depth in nature. In experiment 2, a dense oceanic slab is attached to the back wall plate, generating an additional slab pull force. In that case, the amount of convergence absorbed is ~20% of the total convergence. The back wall slab subducts down to approximately two-thirds of the box, equivalent to 400–450 km depth in nature.

More than one-half of the convergence is absorbed by thickening of the plates. The thickening of the back wall plate varies little, between 131% and 142%, absorbing 16%–18% of convergence, not depending on the amount of subduction. The thickening of the upper plate varies more, between 143% and 200%, absorbing between 17% and 25%, depending on the amount of subduction and of the viscosity of the plate.

The viscous strength of the silicone plate allows the transmission of tectonic forces far from the collision front (Fig. 3). Such transmission favors the formation of a wide and thick plateau. The convergence is partly absorbed by collisional subduction inside the overriding plate, allowing a discontinuity in the thickening between the upper plate and the back wall plate (Fig. 4).

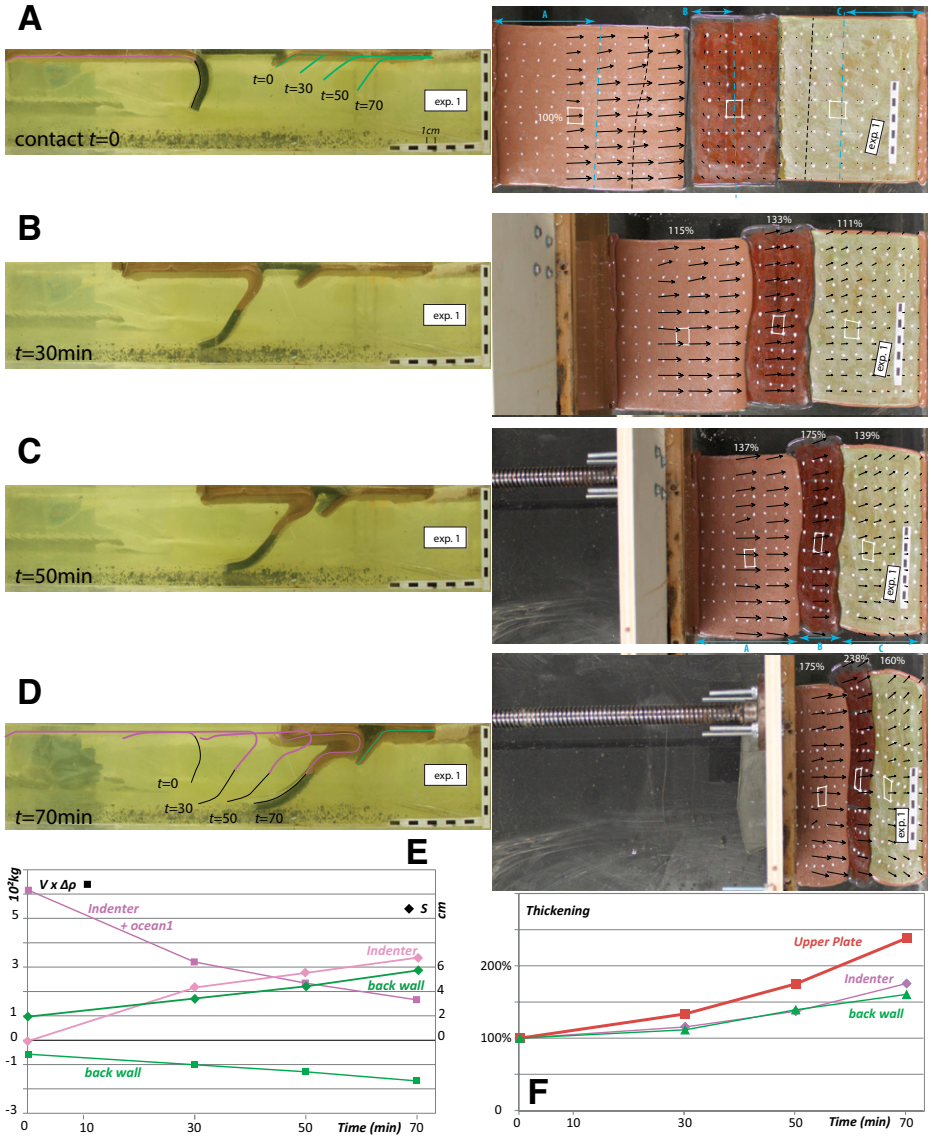

Figure 3. A–D: Side and top view photos of reference experiment (exp.) 1. Side views show successive position of back wall (green), indenter (pink), and ocean (black) slabs. On top view at time t = 0, blue dotted line and blue arrows show the length of plates at t = 50 min. Black dotted line delimits the amount of plate subducted. E: Amount of subduction (*S*, diamond) measure on top view, used to calculate $V \times \Delta\rho$ between slab and mantle (volume slab [*V*] = *S* × thickness plate, square) for the indenter plate (pink) and the back wall plate (green). F: Thickening during the experiment of the white squares drawn on top view.

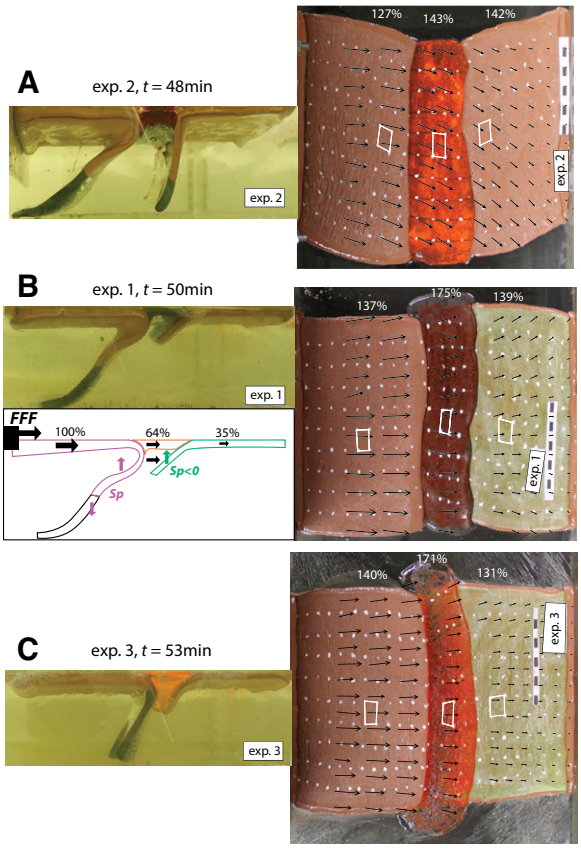

Figure 4. Side and top views photos of experiments (exp) 1 and 2 (ocean 2 attached to back wall plate), and 3 (more deformable upper plate), with the same final length, showing the subduction of the back wall continental plate. For reference experiment 1, sketch of the forces (FFF—far-field forces, modeled by the piston; Sp—slab pull) showing the horizontal tectonic forces transmitted to the back wall plate through the indenter and the upper plate at the surface (black arrows showing the velocity decrease from the piston to the back wall), and by the advancing indenter slab through the mantle at shallow depth. In white on top view, squares were used to estimate the thickening (value in white).

COLLISIONAL SUBDUCTION OF ASIAN CONTINENTAL LITHOSPHERE BELOW PAMIR AND TIBET

The Asian lithosphere subducting southward beneath Pamir reaches at least 250 km (Sippl et al., 2013), possibly 400 km (Negredo et al., 2007), and ~300 km in central Tibet (Kind et al., 2002). A similar amount is estimated for the Asian slab beneath Qiangtang during the early collision (DeCelles et al., 2002) (Fig. 1). Global tomography confirms that the Asian slabs are not attached to any deep oceanic slab (Fig. 1) (Replumaz et al., 2013). Our reference experiments show that such subduction of a continental lithosphere lighter than the mantle is possible in a context of collision with strong far-field forces. This occurs along a suture zone, as it is observed in Tibet (Fig. 1), and the subducted continental lithosphere shows dip and depth similar to that of the natural prototype (Fig. 3).

By comparing the estimation of the convergence during the collision, ~2200 km using the position of the Tethys slab in the lower mantle (Replumaz et al., 2013), with the length of the slab subducting beneath central Tibet or Pamir (250–400 km), we conclude that collisional subduction accommodates between 11% and 18% of the convergence during this episode. It is similar to the amount absorbed in the reference experiment 1 (13%). Adding a first episode of collisional subduction during the early collision, the amount of convergence absorbed by collisional subduction could be doubled.

The Moho below Tibet is as deep as 70 km in the south of the Bangong suture and ~60 km south of the Jinsha suture (e.g., Kind et al., 2002), showing the doubling of the Asian crust during the collision. It is similar to what was measured in our experiments 1 and 2, with a thickening of the upper plate between 170% and 200%, and a discontinuity of the thickening at the suture. Nevertheless, our experiments do not adequately reproduce the thickening process of the Tibetan upper crust (e.g., DeCelles et al., 2002), but rather a distributed ductile thickening by pure shear.

Therefore our experiment 1 reproduces adequately the observations, Asian slab length, amount of convergence absorbed, and thickening of the upper plate, which leads us to conclude that it reproduces adequately the physics of the Asian continental lithosphere subduction. The engine of this process is the horizontal tectonic forces generated by the far-field forces. It is a key process in forming a wide continental plateau in a collision context, such as that of the Tibetan Plateau.

ACKNOWLEDGMENTS

This work has been supported by a grant from LabEx OSUG@2020 (Laboratoires d'Excellence, Observatoire des Sciences de l'Univers de Grenoble; Investissements d'avenir–ANR10 LABX56) and the ANR DSP-Tibet (Agence Nationale de la Recherche de France, Probing Deep and Surface Processes in Central Tibet: ANR-13-BS06-0012-01).

REFERENCES CITED

Bajolet, F., Replumaz, A., and Lainé, R., 2013, Orocline and syntaxes formation during subduction and collision: Tectonics, v. 32, p. 1529–1546, doi: 10.1002/tect.20087.

Becker, T.W., and Faccenna, C., 2011, Mantle conveyor beneath the Tethyan collisional belt: Earth and Planetary Science Letters, v. 310, p. 453–461, doi:10.1016/j.epsl.2011.08.021.

Capitanio, F.A., Replumaz, A., and Riel, N., 2015, Reconciling subduction dynamics during Tethys closure with large-scale Asian tectonics: Insights from numerical modeling: Geochemistry Geophysics Geosystems, v. 16, p. 962–982, doi:10.1002/2014GC005660.

DeCelles, P.G., Robinson, D.M., and Zandt, G., 2002, Implications of shortening in the Himalayan fold-thrust belt for uplift of the Tibetan Plateau: Tectonics, v. 21, p. 1062, doi:10.1029/2001TC001322.

Faccenna, C., Becker, T.W., Conrad, C.P., and Husson, L., 2013, Mountain building and mantle dynamics: Tectonics, v. 32, p. 80–93, doi:10.1029/2012TC003176.

Forsyth, D., and Uyeda, S., 1975, On the relative importance of the driving forces of plate motion: Royal Astronomical Society Geophysical Journal, v. 43, p. 163–200, doi:10.1111/j.1365-246X.1975.tb00631.x.

Kind, R., et al., 2002, Seismic images of crust and upper mantle beneath Tibet: Evidence for Eurasian plate subduction: Science, v. 298, p. 1219–1221, doi:10.1126/science.1078115.

Kufner, S.-K., et al., 2016, Deep India meets deep Asia: Lithospheric indentation, delamination and break-off under Pamir and Hindu Kush (Central Asia): Earth and Planetary Science Letters, v. 435, p. 171–184, doi:10.1016/j.epsl.2015.11.046.

Negredo, A.M., Replumaz, A., Villasenor, A., and Guillot, S., 2007, Modeling the evolution of continental subduction processes in the Pamir-Hindu Kush region: Earth and Planetary Science Letters, v. 259, p. 212–225, doi:10.1016/j.epsl.2007.04.043.

Replumaz, A., Guillot, S., Villaseñor, A., and Negredo, A.M., 2013, Amount of Asian lithospheric mantle subducted during the India/Asia collision: Gondwana Research, v. 24, p. 936–945, doi:10.1016/j.gr.2012.07.019.

Sippl, C., Schurr, B., Tympel, J., Angiboust, S., Mechie, J., Yuan, X., Schneider, F.M., Sobolev, S.V., Ratschbacher, L., and Haberland, C., 2013, Deep burial of Asian continental crust beneath the Pamir imaged with local earthquake tomography: Earth and Planetary Science Letters, v. 384, p. 165–177, doi:10.1016/j.epsl.2013.10.013.

van Hinsbergen, D.J.J., Steinberger, B., Doubrovine, P.V., and Gassmoeller, R., 2005, Acceleration and deceleration of India-Asia convergence since the Cretaceous: Roles of mantle plumes and continental collision: Journal of Geophysical Research, v. 116, p. B06101, doi:10.1029/2010jb008051.

Manuscript received 22 June 2016
Revised manuscript received 1 September 2016
Manuscript accepted 2 September 2016

Printed in USA